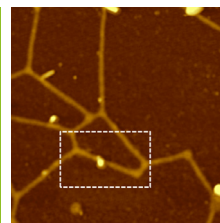


AFM-Raman

TERS Characterization of Lipid Nanotubes as Carbonaceous Material for Electrodes

Application Note

Lipid nanotubes nanoelectronics AFM25



Jana Kalbacova^{1,2}, Kristina Jajcevic³, Ashlin Mario Sequeira³, Dietrich R. T. Zahn², and Kaori Sugihara^{3,4}

¹HORIBA Jobin Yvon GmbH, Neuhofstr. 9, 64625 Bensheim, Germany

²Semiconductor Physics, Chemnitz University of Technology, 09107 Chemnitz, Germany

³Department of Physical Chemistry, University of Geneva, Quai Ernest Ansermet 30, 1211 Geneva 4, Switzerland

⁴Institute of Industrial Science, The University of Tokyo, 4-6-1 Komaba Meguro-Ku, Tokyo 153-8505, Japan

Abstract: This application reports on TERS characterization of lipid nanotubes (LNTs) used as a carbon template for the fabrication of nanostructures. To the best of our knowledge, these LNTs are the smallest surface-patterned organic templates. TERS mapping enables identification of the chemical signature of the LNTs with a spatial resolution of tens of nanometers.

Keywords: Lipid nanotubes, organic template, electrodes, pyrolysis, Raman spectroscopy, tip-enhanced Raman spectroscopy.

Context and Issues

For thirty years there has been research carried out on carbonization of 3D structures to be employed in electronic applications[1]. These structures are prepared using lithography followed by pyrolysis. However, even with state-of-the-art lithography and etching, the structure feature size cannot be reduced below 100 nm[2]. To be able to create even smaller structures it is necessary to shift from a top-down to a bottom-up approach.

Ideal candidates are naturally occurring structures such as DNA fibers[3] or lipid nanotubes[4]. The latter can achieve sizes down to 19 nm in diameter for single-wall lipid nanotubes which is the smallest structure size used for pyrolysis. An additional advantage is their possible alignment on substrates by microfluidics or a glass pipette connected to a manipulator.

Further research into the structuring and the pyrolysis processes is required for the integration of such nanostructures into new electronic devices.

Potential / Input from technique

Raman spectroscopy provides important information about the chemical composition of materials. However, even with the best optics, we can only laterally resolve structures within the diffraction limit, i.e. about a couple of hundred

nanometers. On the other hand, with tip-enhanced Raman spectroscopy (TERS) the diffraction limit can be overcome so that nanostructures can be chemically characterized with a spatial resolution of tens of nanometers[5]. The added value of TERS is the simultaneous use of atomic force microscopy (AFM) providing the topographic information of the nanotubes.

Starting point, what is known?

Raman spectroscopy was used to characterize lipid blocks, before and during the different stages of the pyrolysis process.

The starting material is the main lipid of bacterial cell membranes, 1,2-dioleoyl-sn-glycero-3-phosphoethanolamine (DOPE). The Raman spectrum of bulk DOPE shows a typical symmetric and asymmetric stretching of CH, CH₂, CH₃ bonds between 2800–3000 cm⁻¹. In the fingerprint region, the bands at 1437 cm⁻¹ and at 1298 cm⁻¹ can be assigned to the bending of CH₂/CH₃ groups and the torsion of CH₂, respectively. The bands at 1733 cm⁻¹, 1654 cm⁻¹, and 1261 cm⁻¹ can be assigned to the stretching of C=O, C=C, and the bending of CH, respectively. The band at 1084 cm⁻¹ can be assigned to the stretching of C-C.

Raman spectra of pyrolyzed lipids consist of D band at ~1350 cm⁻¹ and G band at ~1590 cm⁻¹. Both bands are typical for carbonaceous materials. The G (graphitic) band

is always present and comes from the in-plane tangential stretching of the carbon atoms in the lattice. The D (defect) band is visible only if defects are present. As such, it is possible to calculate the ratio of the bands intensities $I(D)/I(G)$ and use it as a relative measure for defects density in the material.

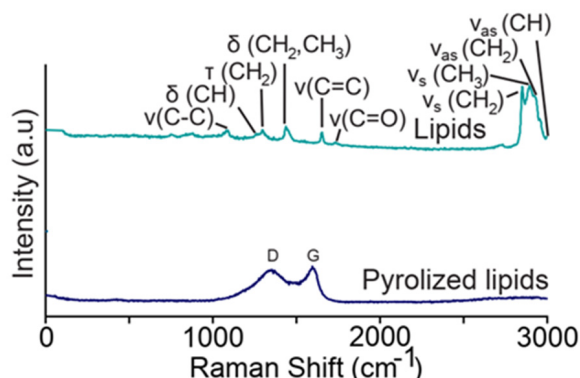


Figure 1: Raman spectra of initial lipids and pyrolyzed lipids.

Table 1: Raman assignment of the bands of the lipid DOPE.

Wavenumber (cm ⁻¹)	Assignment
2999	$\nu_{as}(\text{CH})$
2929	$\nu_{as}(\text{CH}_2)$
2895	$\nu_s(\text{CH}_3)$
2851	$\nu_{as}(\text{CH}_2)$
1733	$\nu(\text{C=O})$
1654	$\nu(\text{C=C})$
1437	$\delta(\text{CH}_2, \text{CH}_3)$
1298	$\tau(\text{CH}_2)$
1261	$\delta(\text{CH})$
1084	$\nu(\text{C-C})$

ν : stretching, ν_{as} : anti-symmetric, ν_s : symmetric, δ : bending, τ : torsion

Description of sample and measurements

Self-assembled lipid nanotubes from DOPE with diameter of 19.1 ± 4.5 nm were deposited onto a silicon wafer and pyrolyzed at 500°C. TERS measurements were performed using a NanoRaman™ system from HORIBA Scientific combining an atomic force microscope (SmartSPM, HORIBA Scientific) with a Raman spectrometer (XploRa Plus, HORIBA Scientific) with a 100× LWD objective with 0.7 N.A. tilted at 60° with respect to the sample plane. A 638 nm *p*-polarized laser was focused onto a cantilever-based silver coated TERS tip with a 0.13 mW power on the sample. With standard μ Raman microscopy the spot size is about ~500 nm. Due to the very low coverage of the lipid nanotubes, no measurable signal could be detected with standard μ Raman microscopy. The sample had to be examined with TERS, where the Raman

signal can be locally enhanced. For further information, the reader may refer to the article by Jajcevic et.al in Nanoscale: Lipid nanotubes as an organic template for the fabrication of carbon nanostructures by pyrolysis [6].

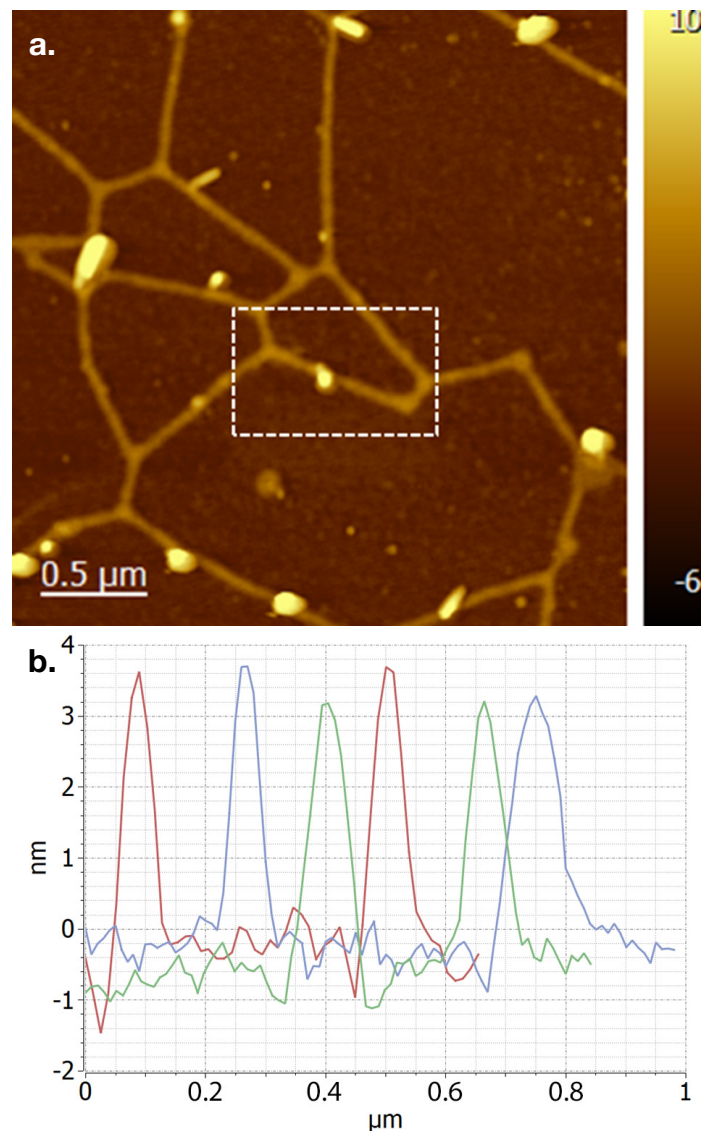


Figure 2: (a) Topographic image with the area indicating the location of the TERS map and (b) Height profiles across lipid nanotubes.

In Fig. 2a, the topography of the sample was examined with standard intermittent-contact mode with a scan size of $3 \mu\text{m} \times 3 \mu\text{m}$. The height of the lipid nanotubes is between 3.5 nm and 4.5 nm (Fig. 2b). The surface of the sample also features larger impurities with sizes typically in the range of 15 – 20 nm.

Within the scanned region, a smaller area of $1 \mu\text{m} \times 0.6 \mu\text{m}$ was imaged with TERS. TERS map consisted of 540 spectra with an acquisition time for each pixel of 20 seconds (total map time ~3 hours). The TERS intensity map of the D and

G band signatures shown in Fig. 3 nicely correlates with the topographic image (Fig. 2a). Also, it is possible to identify a disconnection of the nanotubes (indicated by the white arrow), where a larger particle is located. A deeper analysis of the D and G bands is helpful to assess the defects/crystallization of the nanotubes after pyrolysis (Fig. 4).

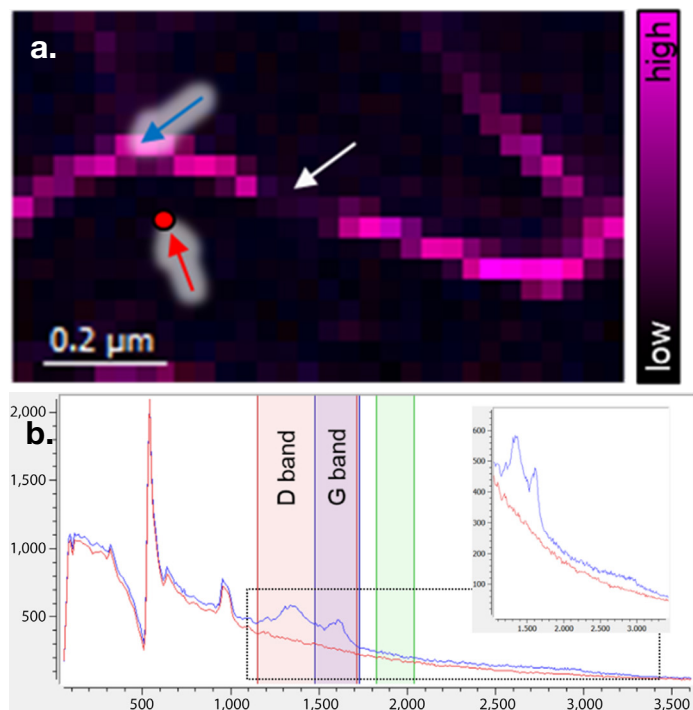


Figure 3: (a) TERS map with integrated intensity of D and G bands. (b) Selected spectra in blue – on the lipid nanotube and red – substrate only. The white arrow indicates a spot with a particle, showing no D or G band signals – the nanotube is disconnected and is thus well correlated with the topography (Fig. 2). One can see in the collected spectra signals from the silicon substrate: sharp band at 525 cm^{-1} and Si 2^{nd} order below 1000 cm^{-1} .

Conclusions and perspectives

In this application note, we have investigated pyrolyzed lipid nanotubes. Since classical μ Raman microscopy was not able to provide sufficient signal and spatial resolution, tip-enhanced Raman spectroscopy was employed instead. Resolution in the nanometer range was achieved allowing the lipid nanotubes to be individually investigated.

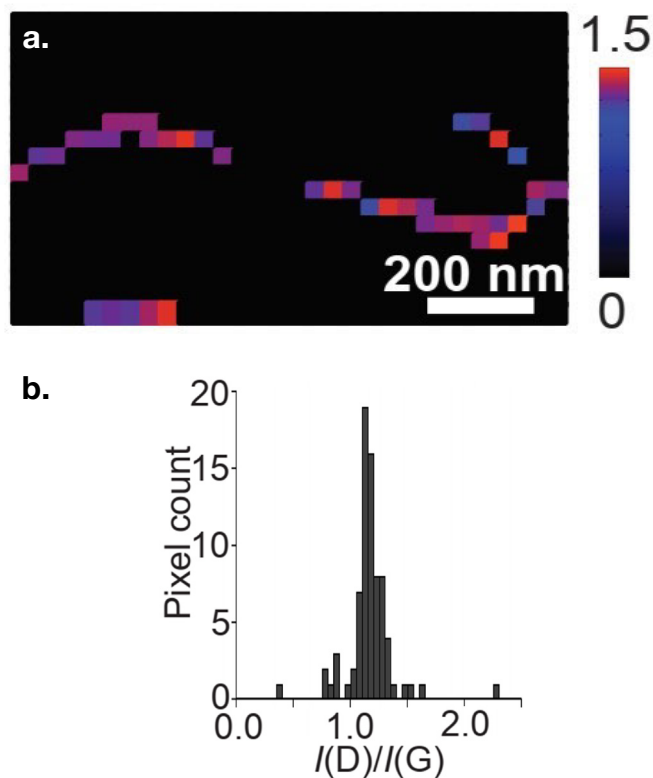


Figure 4: (a) D to G band intensity ratio showing different degrees of crystallization/defects. (b) Corresponding statistics.

References

1. [O. J. A. Schueller, S. T. Brittain, C. Marzolin, G. M. Whitesides, Chem Mater 9, 1399-1406 \(1997\).](#)
2. [G. Seniutinas, A. Webe, C. Padeste, I. Sakellari, M. Farsari, C. David, Microelectron Eng 191, 25-31 \(2018\).](#)
3. [H. Nakao, S. Tokonami, Y. Yamamoto, H. Shiigi, Y. Takeda, Chem Commun 50, 11887-11890 \(2014\).](#)
4. [K. Jajcevic, M. Chami, K. Sugihara, Small 12, 4830-4836 \(2016\).](#)
5. [N. Kumar, B.M., Weckhuysen, A.J., Wain, et al., Nat Protoc 14, 1169-1193 \(2019\).](#)
6. [K. Jajcevic, A. M. Sequeira, J. Kalbacova, D. R. Zahn, & K. Sugihara, Nanoscale 13\(14\), 6927-6933 \(2021\).](#)